The Pennsylvania State University

The Graduate School

College of Engineering

CARBON NANOTUBE FLOW SENSORS:

A COMPREHENSIVE STUDY

A Thesis in

Electrical Engineering

by

Rajaram Narayanan

Submitted in Partial Fulfillment
of the Requirements
for the Degree of

Master of Science

August 2011

The thesis of Rajaram Narayanan was reviewed and approved* by the following:

Theresa Mayer
Professor of Electrical engineering
Thesis Co- Advisor

Srinivas Tadigadapa
Professor of Electrical engineering
Thesis Co-Advisor

Siyang Zheng
Assistant Professor of Bioengineering
Thesis Co- Advisor

Kultegin Aydin
Professor and Head of Electrical Engineering

*Signatures are on file in the Graduate School

ABSTRACT

It has been established that flow of fluids over Carbon Nanotubes (CNTs) generate voltages. The “Sood effect” as it is colloquially referred to, can spawn a myriad of applications when used in conjunction with microfluidic systems. The focus of this project is to develop and design CNT thin film flow sensing devices with different electrode configurations which are robust and highly sensitive. The capability of CNT flow sensors to detect biomolecules has been investigated.

TABLE OF CONTENTS

LIST OF FIGURES.....v

LIST OF TABLES.....vi

ACKNOWLEDGEMENTS.....vii

Chapter 1 Microfluidic Flow Sensors- A brief review.....1

Chapter 2 CNT flow sensors- A review of prior art.....3

Chapter 3 A brief overview of proposed theories……..7

Chapter 4 Device fabrication and characterization……..10

A) Fabrication……....……10

B) Characterization…….14

Chapter 5 Flow sensor testing……..17

A) Testing Protocol……17

B) Results and Discussion- The Pad Electrode……..18

C) Hydrochloric acid conc. analysis on interdigital electrodes.....21

D) Resistance analysis……23

E) Voltage Vs. Flow Rate- Biomolecular studies……..26

Chapter 6 Summary……...31

References 33

Appendix……34

1. LabVIEW Block Diagram.....34

2. Material Specification.....35

3. PDMS Protocol……...36

4. Time trace of flow generated voltage, SNR……...38

LIST OF FIGURES

Figure 1 Physical priciples behind flow sensor. 1

Figure 2 CNT flow sensor- S.Ghosh et al. 4

Figure 3 PDMS-CNT composite flow sensor. 5

Figure 4 Pulsating ratchet driven directed transport. 7

Figure 5 Direct dragging a carriers due to ions……9

Figure 6 Pad and Interdigital electrode configuration…….11

Figure 7 PDMS with microchannels…….....12

Figure 8 Process flow……...…….13

Figure 9 SEM image of 80 Ohm CNT film……..15

Figure 10 SEM image of 60 Ohm CNT film……..……..15

Figure 11 SEM image of 40 Ohm CNT film…….16

Figure 12 Voltage vs. Flow rate for different electrolyte conc……..20

Figure 13 Voltage vs. Flow rate on a 72 Ohm IDE sensor ….……..23

Figure 14 Voltage vs. Flow rate- Resistance analysis……25

Figure 15 Voltage vs. Resistance for a given flow rate…….…….26

Figure 16 Voltage Vs. flow rate for BSA detection…….…..…….28

Figure 17 Voltage Vs. BSA concentration…….……..29

LIST OF TABLES

Table 1: CNT thin film Resistance change due to Protein adsorption……27

ACKNOWLEDGEMENTS

The author would like to express his sincere thanks to Dr. Siyang Zheng for his support throughout this endeavor. It was his constant words of encouragement and mentoring that brought this project to it's fruitful completion. The author gratefully acknowledges Dr. Theresa Mayer and Dr. Srinivas Tadigadapa for their helpful feedbacks that helped shape this thesis.

The author acknowledges Dr. William Hancock and his graduate students Shankar and Yalei and lab tech Dave for their assistance with the centrifugation process.

The support of my lab members Tim, Ramdane, Mingda, Waleed and Ravi has been nothing short of marvelous. The author would like to express his sincere thanks to them for their support.

The author will, forever be indebted and grateful to his parents Mr. Narayanan and Mrs. Rajeshwari for their love, sacrifices and motivation.

The author wishes to acknowledge the entire Penn State community for all the good memories and support.

Chapter 1
Microfluidic Flow sensors- A brief review

Flow measurement is an integral part of sensing technology. The principles of the operation of flow sensors incorporate several aspects of physics [1] (Fig 1). The vast market for microfluidic sensing systems opens up new avenues to explore in the sensing realm from a flow sensing perspective.

The miniaturized geometry of the microfluidic systems gives them an edge over classical sensing technologies in terms of sensitivity, low energy consumption and reliability.

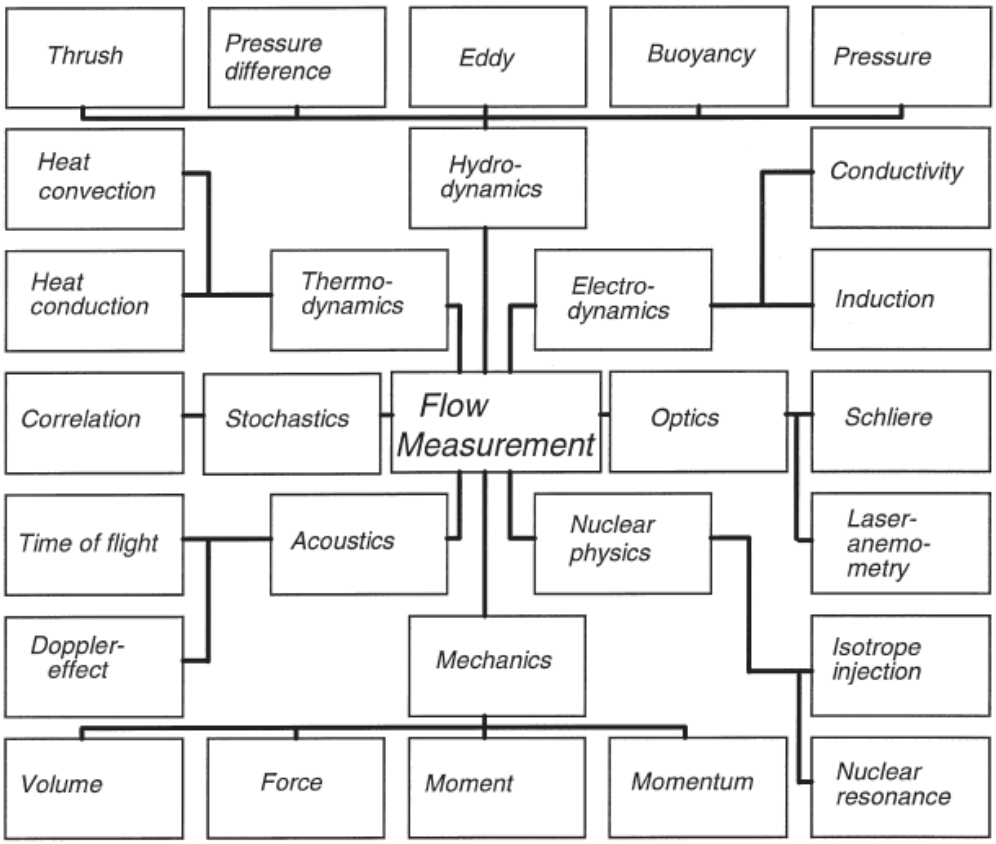

Fig 1: Physical principles behind flow sensing [1]

The ability to measure flow rate using minute fluid volumes will influence emerging lab on a chip technologies significantly. In microfluidic flow sensing technologies, flow sensing can provide information on heat transfer detection [2,3], molecular sensing [4], atomic emission detection [5], streaming potentials [6], electrical impedance tomography [7] and periodic flapping motion [8].The dynamics arising in microfluidic systems provide opportunities for interesting applications. However, in the present biosensing paradigm, where extremely low concentrations are to be measured, extreme miniaturization and a suitable platform to sense these molecules must be established. In this case, miniaturizing classical microfluidic systems is not a good idea considering excessive noise, impaired efficiency in measuring low concentrations of analytes and reliability.

Carbon Nanotubes (CNTs), on the other hand have diameters of the order of nanometers which makes them ideal candidates for biomolecular detection and at the same time CNTs can have lengths of the order of microns which makes it easier to incorporate them with conventional microfluidic systems.

CNT flow sensors [9], the principle theme of this work, are capable of "generating" voltages due to a fluid flow. The following work serves to explore the potential of CNT flow sensors besides the obvious choices i.e flow sensing and energy harvesting. CNT integrated systems show excellent signal to noise ratio (SNR) , their geometry is highly suited for miniaturization and are capable of detecting very low concentrations of biomolecules. The CNT flow sensor's ability to generate voltages on their own without auxiliary power along with the other excellent features discussed thus far make them ideal candidates for implantable continuous monitoring systems. This report does not explore the intensive technologies necessary to engineer a CNT flow sensor based continuous monitoring system. However, their potential for such applications is empirically explored and the data obtained may serve to be a tool when the time arises for these to mature into marketable technologies.

Chapter 2

CNT Flow Sensors- A review of prior art

Carbon Nanotubes (CNTs) have been extensively researched in an effort to understand their novel mechanical, thermal, chemical and mechanical properties. Their immense potential for applications is constantly being explored as they have been integrated with electronics, actuators and sensors. CNTs are 1-dimensional hollow tubes with nothing but a surface.
In his seminal paper, Dr. Sood [9] has demonstrated the possibility of generating voltages across CNTs by flowing fluids over them. In this work, CNT thin films have been fabricated and integrated with microfluidic systems. Devices of varying film thickness and electrode geometries were constructed. The voltage generation potential of these devices was tested by varying parameters such as electrolyte concentration, resistance and analyte (protein) concentrations. Finally, protein detection was performed using these CNT flow sensors to gauge their capability to perform as biosensors that can be integrated into microfluidic continuous monitoring systems.

There is very little literature on CNT flow sensors apart from the work done by Ghosh et. al. Since its first demonstration there has been considerable debate over the underlying theory responsible for this effect. Originally, it was proposed that the asymmetrical pulsating ratchet potentials caused by the shearing of the flowing liquid close to the fluid-CNT interface was responsible for the carrier movement in the CNTs. This theory however was preceded by 2 theories suggested by Kral et al.[10] One of them is that the ions in the fluid directly dragged the carriers along the CNTs causing a current and hence a voltage drop. The second theory is that the fluid motion close to the CNT fluid interface resulted in a momentum transfer between the liquid molecules and the carriers in the CNTs via acoustic phonon generation. Succeeding Dr.Sood's

interpretation was the stick slip model proposed by Persson et al. [11], wherein, the motion of the liquid along the CNT-fluid interface has been described to be of a “Stick Slip” nature resulting in the sublinear and saturating voltage generations for increasing flow rates. Ghosh et al., themselves have encouraged further investigation into the problem and have also expressed their intentions to explore the potential applications of such sensors.

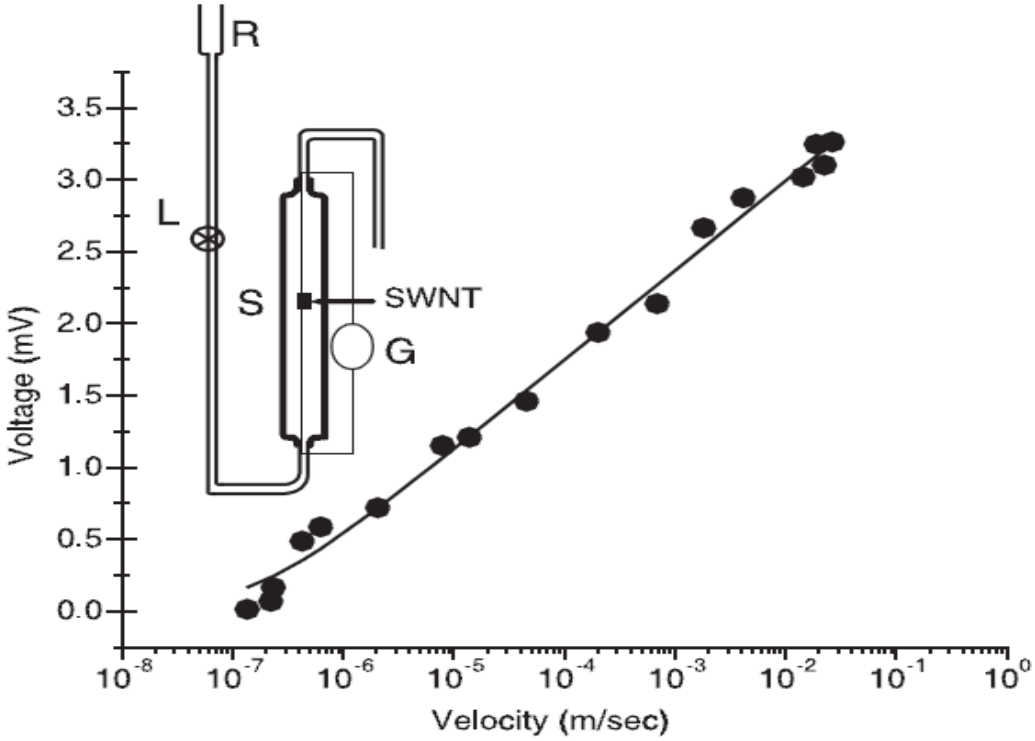

Fig 2: CNT flow sensor (inset- schematic) characteristic [9]

So far, there has been only one report of integrating these CNT flow sensors in a microfluidic system.

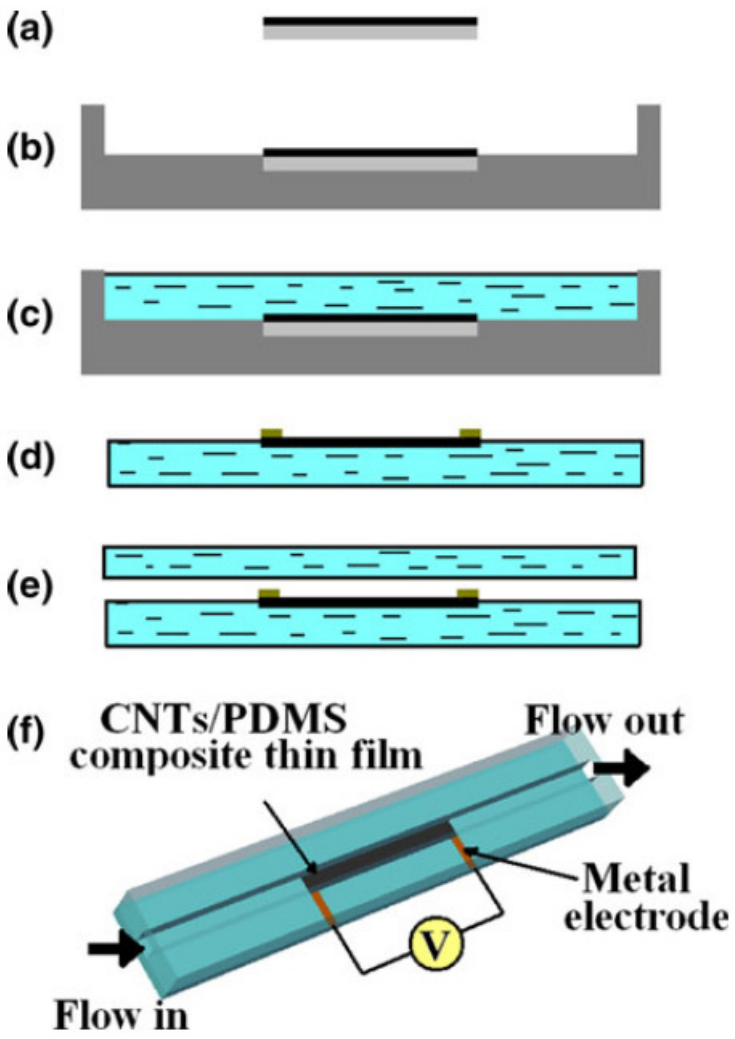

Fig 3: CNT-PDMS composite flow sensor a) Extract CNTs with filter membrane. b)Place membrane on mold. c) Pour PDMS over mold d) Peel off PDMS and deposit electrode metal e) Bond cured PDMS on top f) Schematic of the flow sensor. [12]

In their work, Cao et al. [12] prepared a CNT mat by vacuum filtering CNT dispersion through a filter membrane. The PDMS (polydimethylsiloxane)-CNT composite was then prepared by pouring uncured PDMS over the CNT mat on the filter. On thermal curing, the CNT mat was embedded in the PDMS and the resulting composite was stripped of the filter membrane. Metal electrodes were bonded to the CNT film and additional blocks of PDMS with microchannels were bonded to the PDMS-CNT composite to create the flow sensors (Fig 6).

After performing tests with water and saline solutions of different concentrations, Cao et al, like Sood et al, observed sublinear, saturating flow generated voltage characteristics. However, they have not investigated the biosensing potential of the flow sensor. Additionally, owing to it's low surface energy, the PDMS surface is not ideal for metal deposition and the stability of the electrodes and subsequently the reliability of the device fabricated by Cao et al. is questionable.

The approach taken throughout the course of this work seeks to construct a reliable and reproducible CNT flow-sensor. Additionally, boundaries have been stretched in exploring for the first time, the biosensing capabilities of these flow- sensors.

Chapter 3

A brief review of proposed theory describing the operation of CNT flow sensors

a) Pulsating Ratchets- S.Ghosh et al [9]

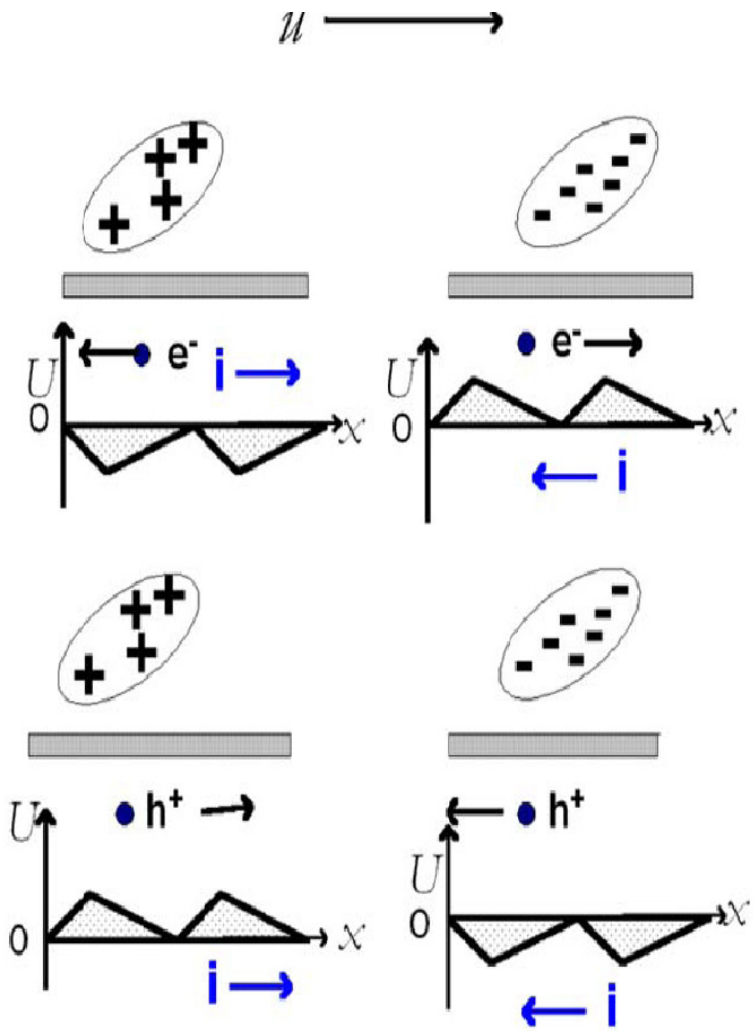

Fig 4: Pulsating Ratchet driven directed transport- S.Ghosh et al [9]

Here the charge carriers in the nanotube experience spatially asymmetric potential arising from, for example, the fluctuating imbalances in the local charge neutrality of the ionic fluid. The asymmetry is provided by the velocity gradient experienced by the ionic charge imbalance in the

fluid at the nanotube-liquid interface. It has been shown that the model based on pulsating ratchets can qualitatively explain the observations. A prediction of the ratchet model is the direction of current with respect to the flow velocity. In a linear response theory based on the viscous drag (the phonon wind) the particle current will have the same direction as the fluid flow velocity U and therefore the sign of the electric voltage and current is determined by the sign of the charge carriers. Thus, for hole-like carriers, the induced current I will be parallel to U, whereas for electrons as carriers, I will be antiparallel to U. On the other hand, for the ratchet model, for a given direction of the ratchet bias, the direction of current will be independent of whether the carriers are holes or electrons. It will depend on the sense of the bias (asymmetry) of the ratchet potential. In a polar fluid of a given ionic strength, both positive and negative ions will be present and the net effect will be determined by the dominant ratchet. This is schematically illustrated in Fig. In Fig, the dominant ratchet is formed by the positive ions and it can be seen that for both the electrons and holes, current is parallel to the flow velocity. In Fig the dominant ratchet is formed by negative ions in the liquid, which gives I antiparallel to U for both types of carriers in the nanotube

b) Phonon Drag and Coulomb Drag- Kral and Shapiro

We now come to discuss the possible mechanisms of flow-induced voltage generation in carbon nanotubes. Kral et al, have discussed theoretically two mechanisms to generate an electric current in a metallic carbon nanotube due to the flowing liquid. One mechanism, termed phonon drag, involves the transfer of momentum from the flowing liquid molecules to the acoustic phonons in the nanotube, which in turn drag free charge carriers in the nanotube. Another mechanism, termed cog-wheel mechanism, involves a direct scattering of the free carriers in the nanotube by the fluctuating Coulomb fields of the ions or polar molecules in the flowing liquid. It has been argued that the phonon drag mechanism gives five orders of magnitude higher current than from the cog-

wheel mechanism. Both mechanisms give linear dependence of generated voltage on the flow velocity.

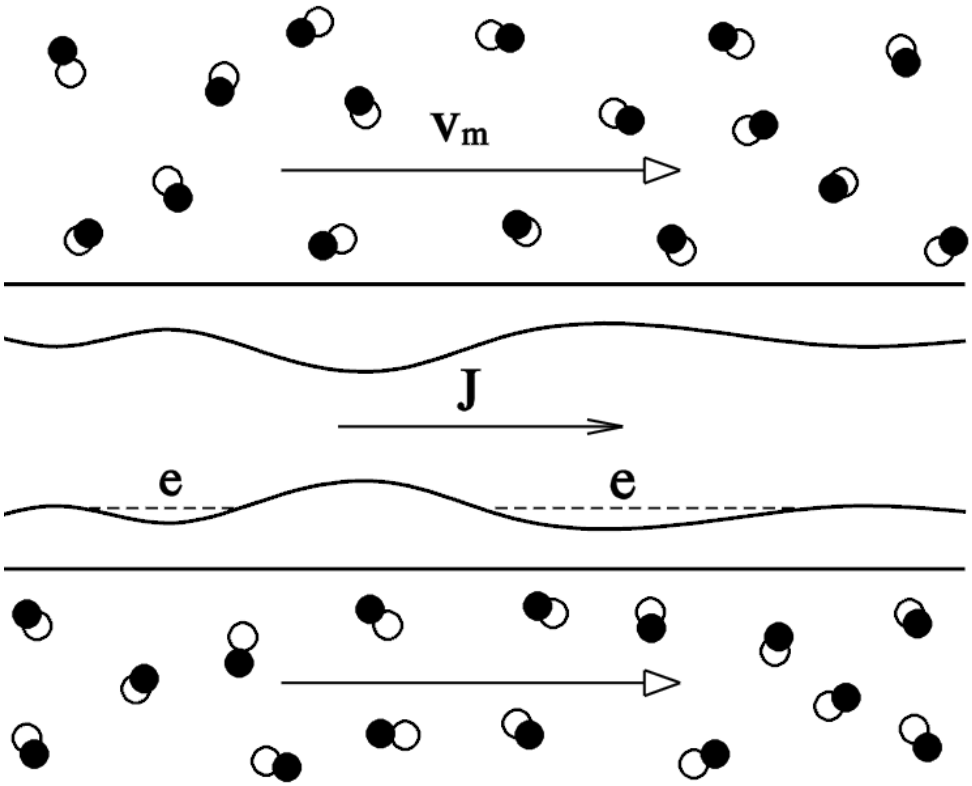

Fig 5: Direct dragging of carriers due to the ionic liquid- Kral and Shapiro [10]

Chapter 4
Device Fabrication and Characterization

a) Fabrication

• CNT dispersion and centrifugation:

CNT thin films on glass used in this work were prepared by a "drop drying" or "drop casting" method. 1% w/vol. Sodium Dodecyl Sulfate (SDS) solution was used as the dispersant. CNT powder (prepared by arc discharge) was added to the dispersant at a concentration of 0.1 mg/ml. The solution was then sonicated for 15 minutes using a tip-type ultrasonicator. Sonication for long periods of time may shorten the CNTs leading to the degradation of it's electronic properties. Post Sonication, the dispersion is then centrifuged at 45000 rpm for 15 minutes. The supernatant was then collected and centrifuged once again at the same period for the same time duration. The centrifuged solution was then transferred to a container and sealed tightly to prevent solvent evaporation and subsequent bundling.

• Substrate details:

Substrates used for CNT drop cast deposition was made of Soda lime glass which was 0.55 mm thick. On the glass substrate, electron beam evaporated chrome/gold electrodes (Cr: 10nm/ Au: 150 nm thick) were deposited. Excess metal was etched off using Au etchant and Cr-7 Cr etchant. The substrates used for all experiments consist of 2 pairs of electrodes (Fig). The substrate was immersed in subsequent baths of pure Acetone and Isoproponal (IPA) to remove the photoresist off the substrate. The substrate was then placed on a hot plate which was maintained at a temperature of 90 deg C.

• Drop cast procedure:

The drop cast procedure was chosen out of possible CNT thin film fabrication procedures such as vacuum filtration [13] and dip coating [14] because of the ease of deposition and low

consumption of raw material. Additionally, vacuum filtration is done using filter membranes (pore sizes ~.4-.5µm) that were made of nitrocellulose (typically) and removing the resulting thin film from these membranes is cumbersome and even after complete dissolution of the cellulose membranes in Acetone, some membrane debris was observed on the films in our case.

A micropipette was used to pipette out small volumes (~10µL) of the CNT dispersion and was transferred to the hot substrate as a "drop" in between the metal electrodes. One must note that it is imperative to make sure that the deposited drop be small as it spreads while solvent evaporation and large drops may allow the spreading to deposit CNTs in the region between the two pairs of electrodes resulting in possible cross conduction. The solvent dries leaving behind a crust of CNTs and SDS, the substrate was then placed in a pure methanol bath for 10 mins to remove the SDS owing to methanol's affinity towards SDS [15]. The process of dropping, drying and SDS removal was repeated several times till a thin film of desired resistance was obtained.

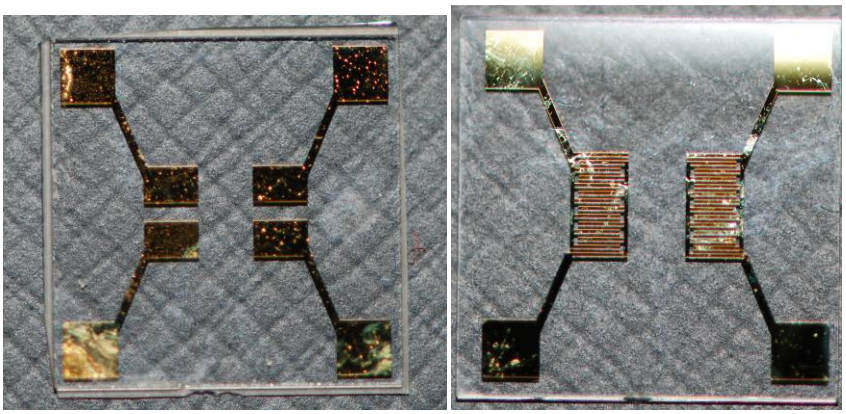

Fig 6: Pad electrode (left) and Interdigital Electrodes (IDE) (right)

The CNT thin film on substrate was then placed in a 1M HCl (hydrochloric acid) bath for 2 hours to remove any catalyst metal and or carbon particles adhered to the CNTs.

- **PDMS device fabrication and bonding:**

PDMS was then prepared using the protocol specified in Appendix A3. The PDMS mould was fabricated using a AZ4620 photoresist mask followed by stepper photolithography

and subsequent DRIE etching. A thin layer of Hexamethyldisiloxane (HMDS) was then coated on the mold by placing a small vial of HMDS on the edge of the mold. The mold and HMDS vial were placed under a chemical hood as the vapors of HMDS are toxic. After coating the mold with HMDS for 10 mins the PDMS is the poured on to the mold. The setup is left in a convection maintained at 70 deg C for 2 hours. The cured PDMS is then stripped off the mold. The dimensions of the microchannel used for the experiments were 9.6 mm in length, 2 mm in width and 50µm in height (Fig).

Holes for fluid inlet and outlet were punched through the PDMS device using a 20 gauge Luer stub adapter. The PDMS was subsequently Sonicated in an IPA bath for 5 mins and the washed with Acetone and dried using an air gun. The glass substrates were rinsed with water and IPA and were dried at 70 deg C. The PDMS block was then bonded quickly to the hot glass such that the channel housed the CNT films on electrode. The bonded chip was then placed in a convection oven at 90 deg C overnight for further bonding.

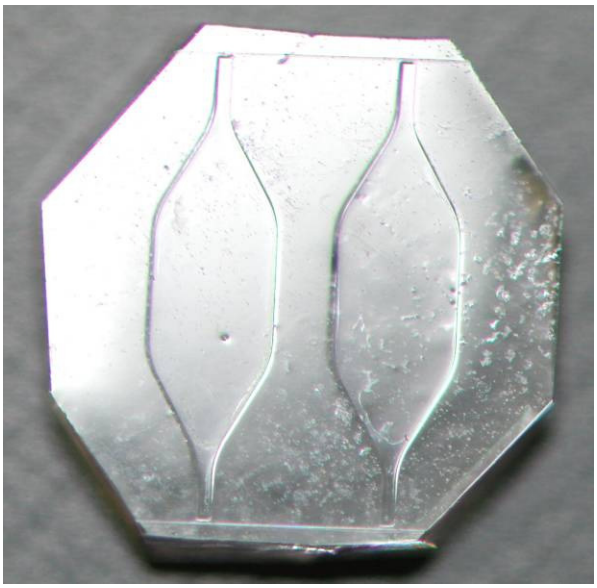

Fig 7: PDMS with microchannels facing up

- **Wire bonding:**

A standard 22 gauge copper wire was then bonded to the device using silver epoxy. The device temperature was maintained at 60 deg C on a hot plate to facilitate the curing of the silver epoxy.

The device was then further protected from potential leaks by coating the edges of the device with uncured PDMS. The silver epoxy which is now exposed to air was also coated with a thin layer of uncured PDMS. This setup was placed in the oven and the temperature was maintained at 70 deg C for 2 hours. The device is now fully protected from leaks; no part of the wiring is exposed to the atmosphere thereby facilitating low noise measurements.

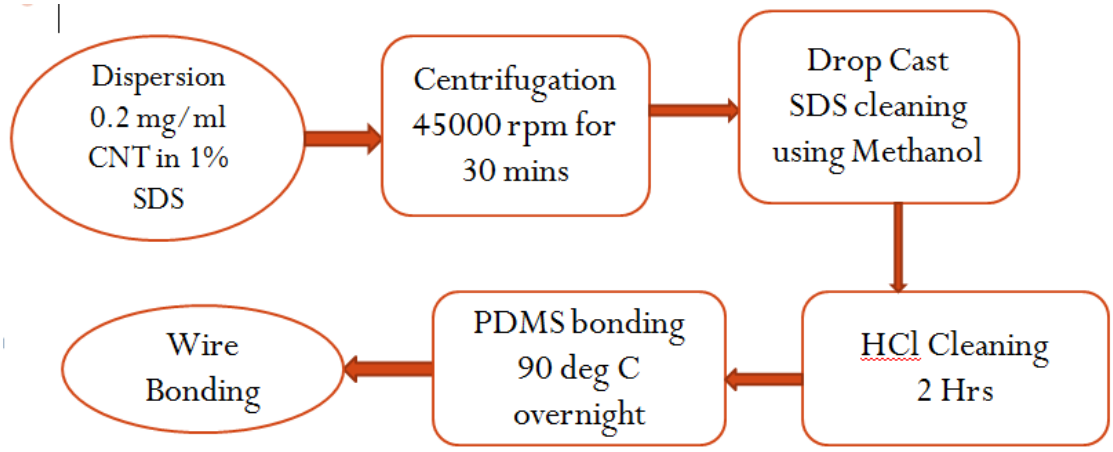

Fig 8: PROCESS FLOW

b) Characterization:

The Scanning Electron Microscope (SEM) pictures of CNT thin films on IDE are shown below. The resistances of the films that were imaged were of 40, 60 and 80 Ohms.

As discussed in the fabrication section, the drop cast process was performed repeatedly until desired resistance values were obtained. It was observed that as the number of deposition cycles increased the resistance of the CNT thin film decreased. CNT thin film networks must be viewed as a percolative network [13]. As we go on increasing the concentration of the CNTs deposited we create more and more conductive paths across the electrodes. As CNTs are conductive, multiple parallel conductive paths serve to decrease the film resistance. From the SEM images one can see that the CNTs are not aligned in a particular direction, i.e. the film is anisotropic. Also, from Fig 9 , it is evident that the deposition is not homogenous. One can see the underlying electrode metal (yellow) and glass (blue) regions at some places rather that others. This is an indication that the density of the CNT network is more in some regions than the other.

Although film homogeneity and anisotropy (CNT alignment) is ideal for any kind of electrical sensor based on CNTs, under our circumstances we decided to keep it simple and try to repeat prior art albeit with a thin film of CNTs. Hence, procedures like dielectrophoretic CNT alignment was not used to obtain anisotropic films. The following experiments can be can be repeated with CNT films fabricated using the abovementioned processes and the author welcomes other groups to try and improve upon the existing protocol and report an overall improvement of experimental data.

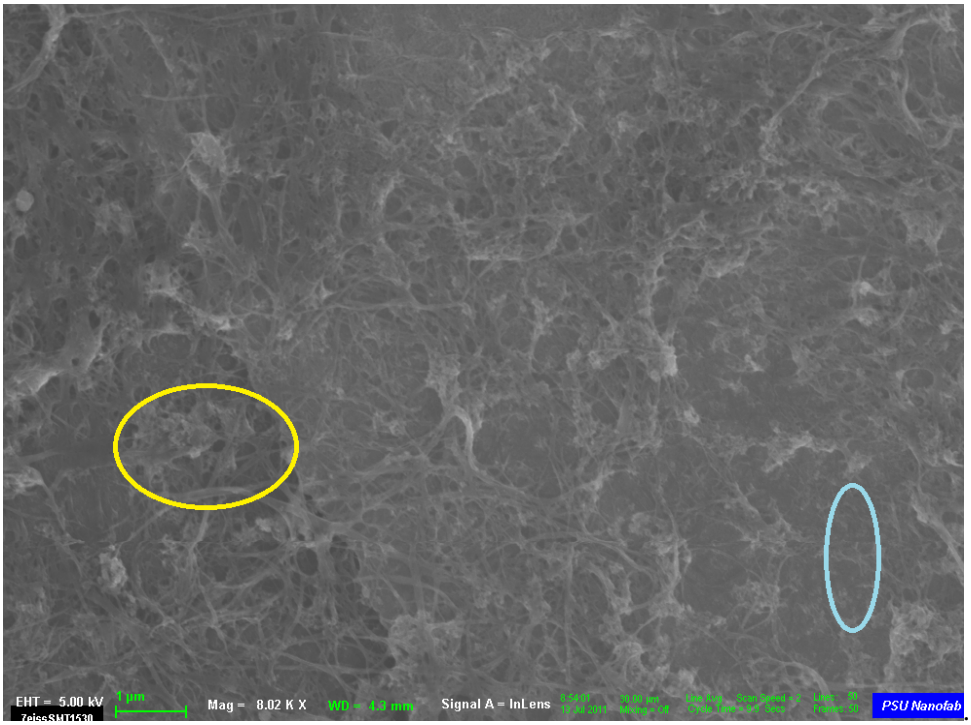

Fig 9: SEM image of an 80 Ohm film. The circled regions depict the underlying electrode (yellow) and Glass (blue) respectively.

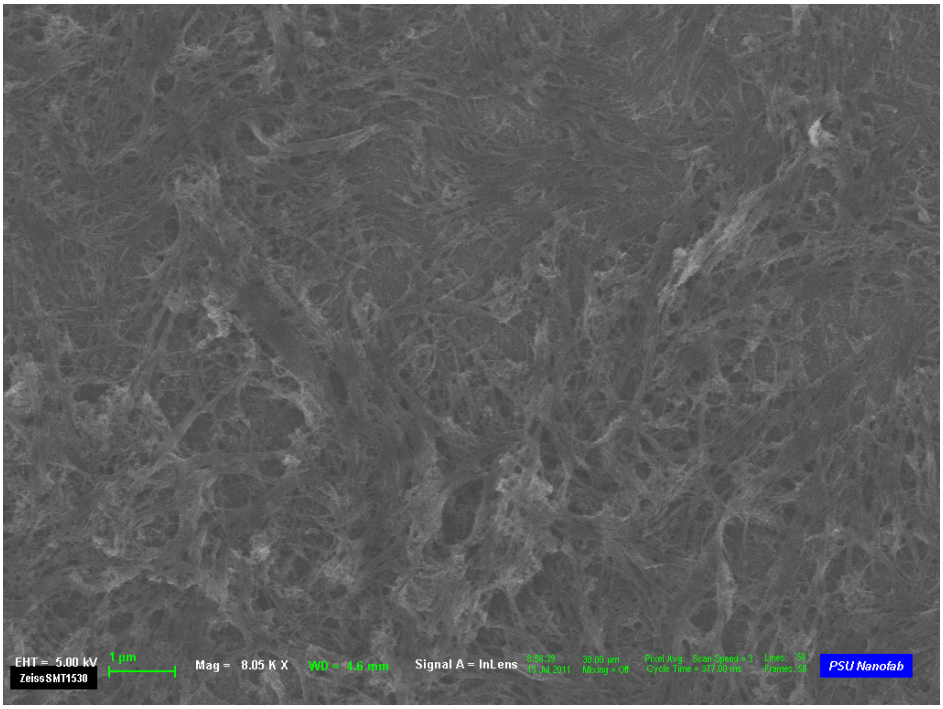

Fig 10 : SEM image of a 60 Ohm film. CNT bundling is evident.

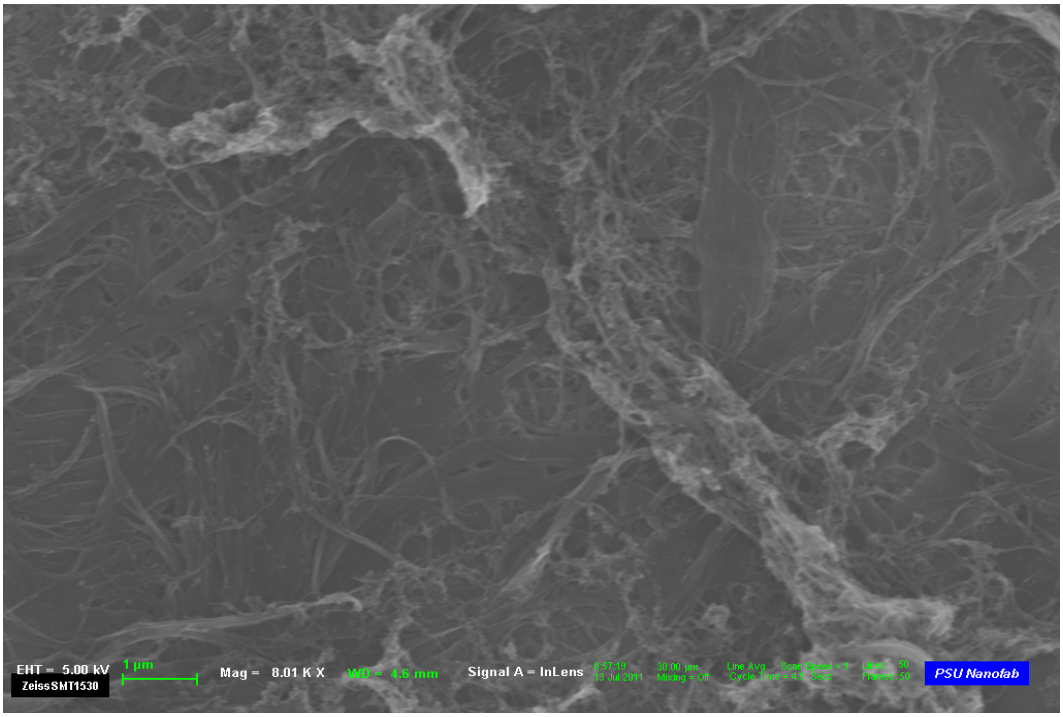

Fig 11: SEM image of a 40 Ohm film. Heavy bundling is evident.

Chapter 5

CNT flow sensor testing

A) Testing protocol

CNT flow sensors have been fabricated on two kinds of electrode configurations namely- Pad type and Interdigital Electrodes (IDE). In this section the general protocol for a microfluidic flow sensor testing has been elucidated. After obtaining some insight into the workings of the flow sensor on both the electrode configurations, one of the electrode configurations is chosen for future experiments and the motivations for doing the same has been provided.

PDMS is inherently hydrophobic [16]. The PDMS devices used for the following experiments have not been treated via oxidation or surfactants to improve wetting owing to the fact that such treatments may interfere with the experiments themselves. Since PDMS are hydrophobic and gas permeable, bubble formation is inevitable when we try to wet them with say DI water. Bubbles are a serious problem when one tries to monitor flow in a device over long periods of time as they may change both flow and temperature profiles radically over the course of the experiments. Vacuum degassing of the device is an option but owing to the high gas permeability of PDMS, it is not possible to completely degas the device thereby sparing small bubbles near channel sidewalls that may serve as a nucleation site for further cavitations during the course of the experiment.

In order to overcome this problem, prior to every flow sensing experiment, the channel was washed with IPA. IPA has low viscosity and hence low surface tension thereby wets the channel fairly well and serves to displace even the minute bubbles from channel edges. The process of bubble elimination was closely monitored under the stereo microscope under 10X magnification

to ensure even the smallest visible bubbles were eliminated. PDMS is also permeable to organic solvents; thereby IPA flushing permeates the PDMS close to the channel walls and creates a barrier against bubbles that may later nucleate. Post IPA flushing, the channel was rinsed thoroughly with DI water and the channel was again monitored under the stereo microscope but no bubbles were apparent this time.

Once the channels have been wetted, the device is placed under DI water in trough. The leads across the test channel were connected to the "Channel 1" leads of the Agilent 34420A nanovoltmeter and the reference channel was connected to "Channel 2". Differential voltage was measured. The voltmeter is also in sync with a data acquisition program created using LabVIEW (National Instruments). The purpose of taking differential measurements is to eliminate any possible thermal noise that originates during and before the experiment commences.

Two 1ml syringes (glass syringes, Hamilton Co.) were loaded with the desired liquid. A syringe pump (KD scientific Pico pump) was used to pump the fluid through an inlet Teflon tubing which was subsequently plugged to the steel tubing that is placed as the inlet to the PDMS microchannels.

At a given time, a single flow rate and the respective output signal was measured. The output was recorded when the signal reached a steady state. All of the flow sensing was done in this manner i.e. in the form of flow pulses rather than continuously changing flow rates in order to monitor base line drifts if any existed. Also, for given electrolyte of given concentration, the flow sensing experiment was repeated thrice to evaluate and repeatability and calculate uncertainties.

B) Results and Discussion- The Pad electrode

CNT flow sensors were tested initially on both Pad electrode configurations and IDE configurations. This was done in part to compare the data obtained in this work to prior art and also to try and gain some insights into the working of these flow sensors.

In Fig 12 flow sensing was done on Pad electrode with different electrolytes of varying concentrations. The electrolytes used for this experiment were pure DI water, Phosphate Buffer Saline solution (PBS, concentrations of 1X (10mM) and 10X) and Hydrochloric Acid (HCl, concentrations of 0.1M and 0.2M). Acids of higher concentrations weren't used purely because they didn't wet the channel very well.

The minimum flow rate used in the experiment was determined by the flow induced voltage obtained for a minimum flow rate of the weakest electrolyte. The convention was then used for all electrolyte concentrations for the sake of uniformity. However, this is not the case for all the experiments done as a part of this work.

Fig 12 reveals some familiar and interesting points.

- The flow induced voltage as a function of flow rate increases at first and then saturates at high flow rates. This was demonstrated by Ghosh et al, the workers who performed the original experiment and this has been further validated by the date presented in this work.
- For a given flow rate, the flow induced voltage increases as a function of the electrolyte concentration.
- One interesting point however is that, in this work, the voltages developed for water and saline solutions are in the negative direction. This is in contradiction with the work of Ghosh et al. [17]. They have experimentally demonstrated that by electrochemically biasing CNT films in an electrolyte (0.01 M KCl in their case) using a counter electrode; they could reverse the polarity of the voltage. In this work no such obvious biasing mechanisms were used. One possible explanation is the effect of the glass substrate. Considering the fact that the flow sensor fabricated as a part of this work were done so by depositing CNTs on glass substrates and that glass attains a net negative charge in DI water and saline media [18], due to the deprotonisation of the silanol group in DI water

and saline media. In acidic media, the glass substrate is reprotonated thereby loses it's negative charge. The charging of the glass substrate could act in a way to bias the CNT films and the electrolyte in contact with it to reverse the potential. However, a concrete theory has not been laid out as to how this might alter the carrier- ion dynamics at the CNT-Fluid interface and extensive experimentation is further required to come up with a theory.

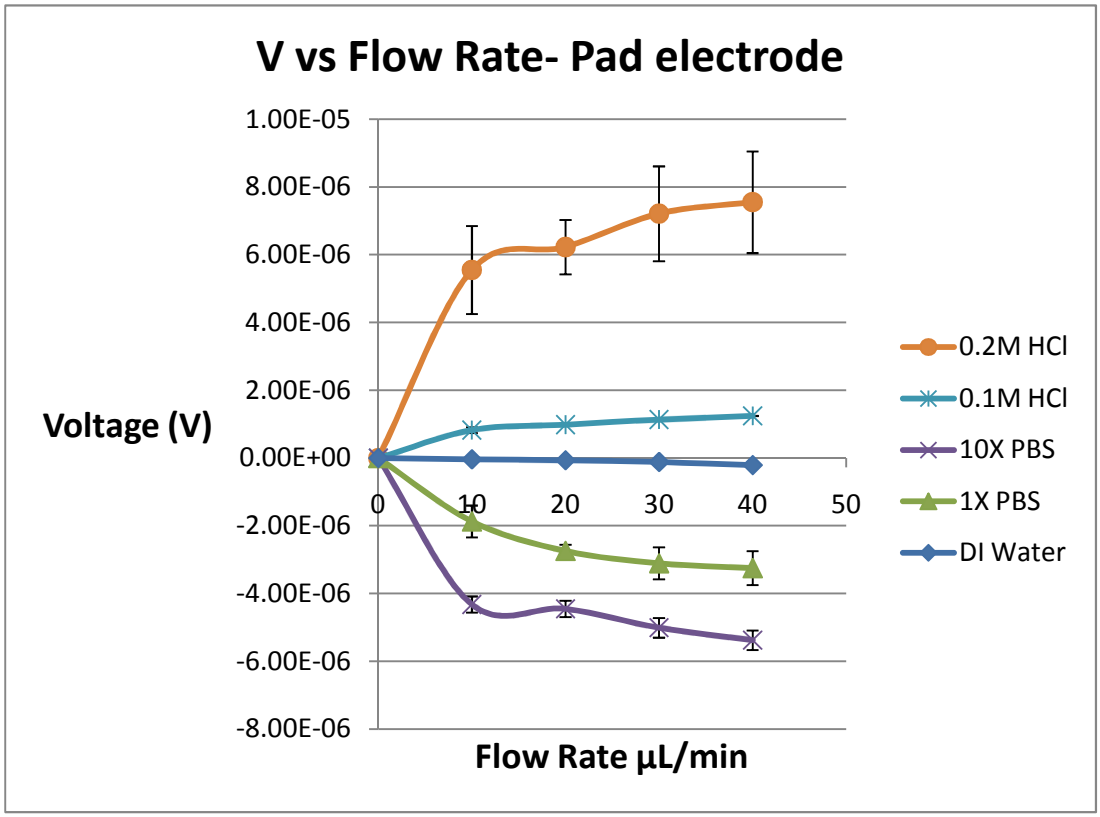

Fig 12: Voltage Vs Flow rate for different electrolytes. Standard deviation calculated based on 3 runs of flow voltage measurement for each electrolyte.

Thus far a tentative explanation for the observance of negative voltages has been provided. The author is yet to explore the possibility of operating the device at it's isoelectric point (the value of pH at which the glass surface has no charge) and other basic (pH > 7) solutions. However, as we can observe from Fig 12 , the relationshipe between electrolyte concentration and flow induced

voltage is non monotonous and for the pad electrode configuration the data obtained for acids of pH 2 and 3 were much lower than that of pH 1 (0.1 M Hcl) had a poor signal to noise ratio. Initial experimentation with basic solutions such as 5% KOH resulted serious modification device resistance over a short course of time leading to unreliable results. The problem will hopefully be addressed soon enough to provide experimental data to validate the abovementioned theory.

C)Hydrochloric acid (HCl) Conc. Analysis on Interdigital Electrodes (IDE)

The "Pad" electrode configuration has allowed the validation of behind the working of the CNT flow sensors. However, considering the goal of the work is to explore the possibilities of using the flow sensor for biosensing, it was necessary to come up with a scheme to reduce th resistance of the CNT thin films to aid sensitive biomolecular detection and to improve the signal to noise ratio (SNR) of the device. Employing the drop cast method on pad electrodes led to an eventual resistance saturation after a few runs and low resistances necessary for biosensing was not achieved.

Interdigital elctrodes (IDE) were comsidered as an alternative to pad electrodes to overcome the aforementioned problem. IDE with their closely placed fingers boosted the conductivity of the CNT film . Very low resistances (~22Ω) were achieved in a limited number of drop cast runs where as the resistance of the films on Pad electrodes eventually saturated at around 200 Ω. As a result, the rest of the work has been carried out entirely using CNT thin films deposited over IDE configuration.

It should be noted that, diluted hydrochloric acid was used as the test fluid for the rest of the study. There are 2 reasons for this choice, they are as follows

1. HCl have a very high K_a, that is they dissociate almost completely in water inturn contributing a large amount of ions to participate in voltage generation.
2. Protein molecules develop a positive charge in acidic media leading to interesting interfacial phenomena during the course of biosensing.

CNT thin film deposited over IDE with a resistance of ~72 Ω was fabricated in order to perform a concentration analysis. Hydrochloric acid of different concentraions was tested in the flow sensor in order to see if there could be developed a relationship between generated volatge and acid concentration (Fig 12).

The flow generated voltages for a device of given resistance and a given flow rate increases for an increase in acid concentration. Qualititatively this could be explained by the fact that higher concentrations of HCl give rise to increased amount of hydronium (H_3O^+) concentration. Since the previous experiment and prior art suggests an increase in flow generated voltage for an increased ionic concentration these results serve to test the electrode configuration as well as validating the conclusions reached by prior art.

However, the relationship between the generated voltage and the concentraion seems to be non-monotonous. So far, no quantitative studies have been done to explain this particular anamoly . For HCl concentrations below 0.01M, there wasn't any discernible signal as was the case with pure water. For concentrations greater than 0.2M HCl, acid wetting within the PDMS microchannel was a massive problem owing to increased surface tension. Non wetting caused spontaneous cavitation within the channels which produced highly irregular, irreproducible results.

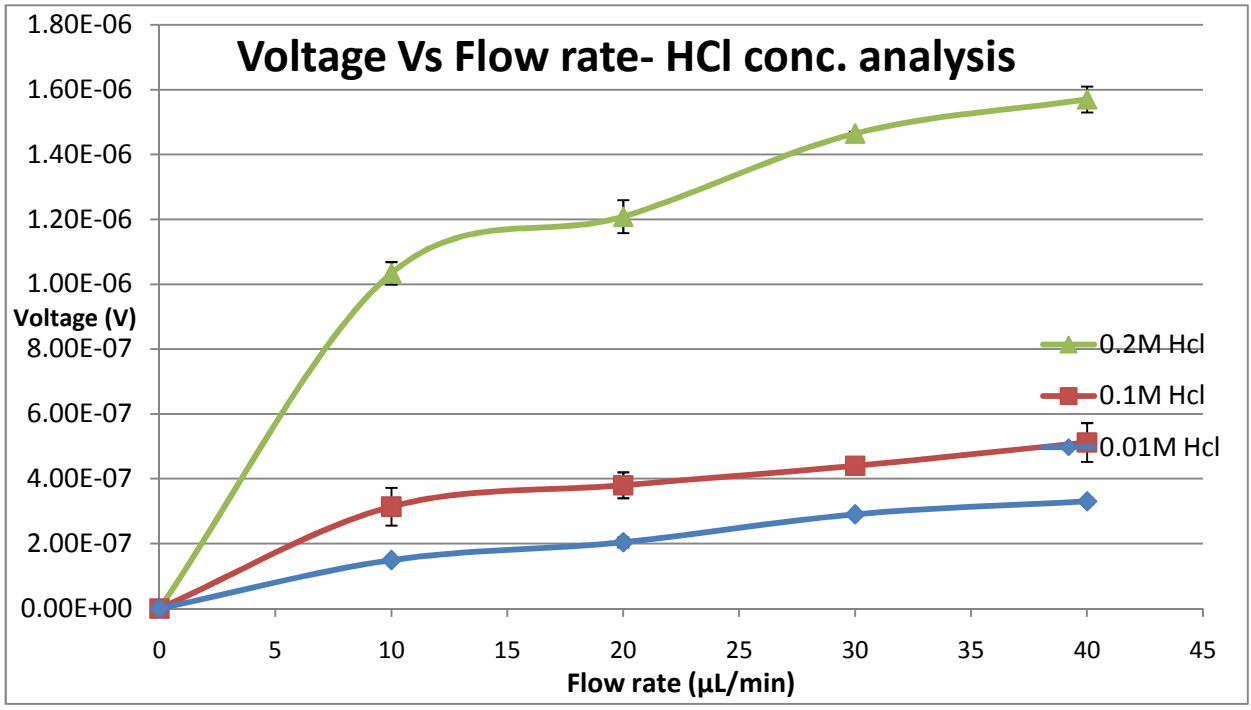

Fig 13: Voltage vs Flow rate on an 72Ω flow sensor. IDE configuration was used as electrodes. A set of 3 experiments for each concentration were run for flow rates 10,20,30 and 40 ul/min for differenct HCl concenrtations.

D) Resistance analysis

Resistance analysis was performed using CNT flow sensors of different resistances (22Ω,44Ω,66Ω and 80Ω). The puprose of performing resistance analysis are three fold:

1. To understand the Voltage vs Resistance characteristics and to verify the linearity of the relation according to Ohm's law. The flowing liquid initially generates a current across the CNT film which appears as a voltage drop that is measured using a voltmeter.

   A flow sensor with linear Voltage-Resistance characteristics points to a reliable device.

2. This experiment was done with biosensing in mind. Protein attachment to CNTs caused an increase in resistance in CNTs due to carrier scattering. The generated flow voltage post protien attachment can be compared with the volatge generated for the corresponding resistance without the protein attachment. This will reveal the interfacial phenomena that takes palce in CNT flow sensors during bio-sensing.
3. Analysis of the voltage drop for different resistance values is helful to explore if the electrokinetic mechanisms such as streaming potential are responsible for flow generated voltages.

At the time when Ghosh et al., published their findings, there were proposals from other groups suggesting that the effect involved was electrokinetic [19] . To date, no one has conducted a resistance analysis on the CNT flow sensors .

Electrokinetic flow generation is a strictly ionic phenomena that does not involve charge carriers within the CNTs. If it was electrokinetic mechanism, the charge neutrality would be violated at the liquid CNT interface due to the formation of an Electrical Double Layer (EDL).

In electroosmotic flow, when a pressure gradient is applied across the length of the microchannel, these counterions move in response forming a streaming current. When the measuring circuit is left open, the build up of counterions on one side of the channel shows a streaming potential.

Streaming potential $V = K\zeta \Delta P$;

K – a material constant including permittivity, viscosity and specific conductivity of the liquid. This is constant for a given liquid.

ζ – Zeta Potential, V

ΔP- Pressure gradient, Pa

Streaming potential is then directly proportional to the Zeta potential. However, when the ionic concentration of the liquid increases, the Zeta potential decreases and hence for increased

ionic concentrations a streaming potential would actually decrease. Our results (Fig 12) and similar data from S.Ghosh et al., show that the measured voltage increases with ion concentration which doesn't agree with the streaming potential theory.

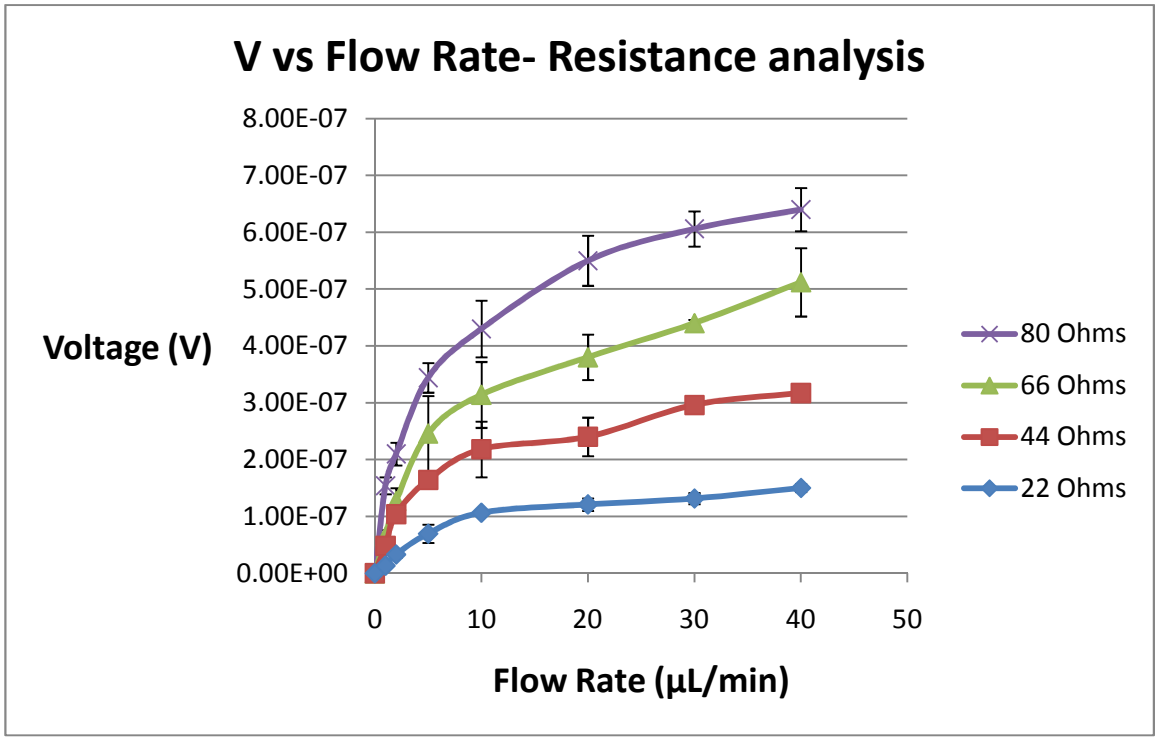

Fig 14: Voltage vs flow rate characteristics for 4 different resistances

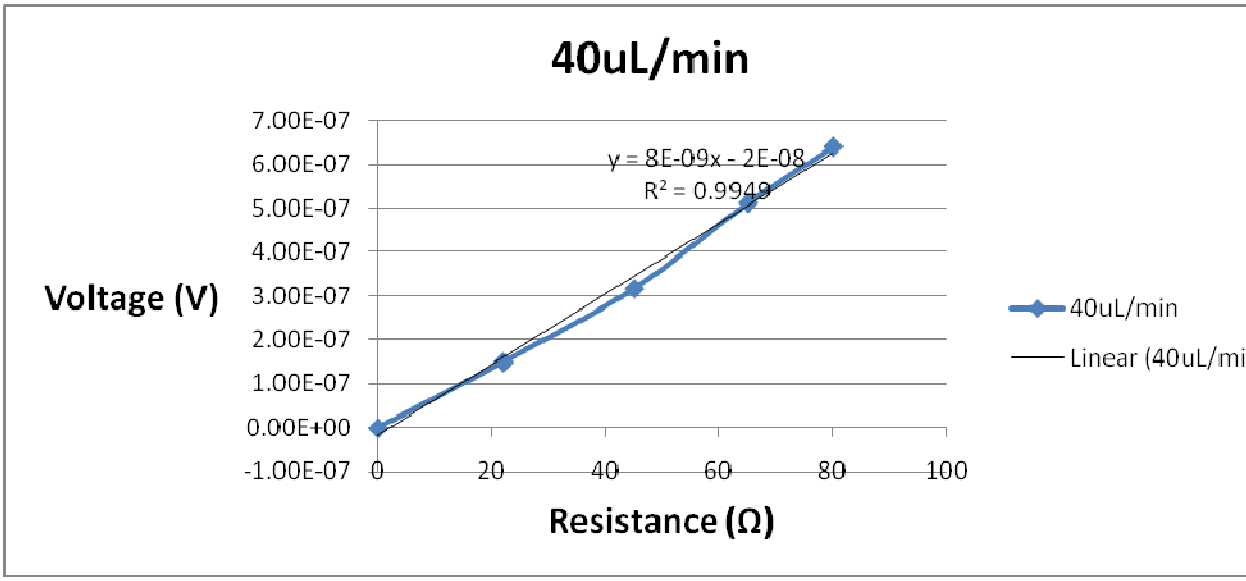

Fig 15: Voltage Vs Resistance for a given flow rate.

In Fig 14, we see that the voltage drop produced due to the fluid flow across the CNT thin film increases with increase in the resistance. This may may indicate that the flow acts as a constant current source. In Fig 15, we can see the linear increase of the voltage drop with respect to resistance.

E)Voltage vs Flow rate Characteristics: Biomolecular studies

The ultimate goal of this work was to test the CNT flow sensor as a biosensor. The flow sensor's potential to detect molecules at the fluid-CNT interface during a constant fluid flow could be harnessed to develop continuous monitoring system to sense a myriad of stimuli both in vivo and in vitro. Besides, the novelty of the idea itself was a great motivation to pursue it.

Considering the fact that this was the first ever attempt to test the flow sensor as a biosensor, a simple hassle free sensing protocol was adopted. Bovine Serum Albumin (BSA) proteins were used in the biosensing experiments.

BSA along with Streptavidin, Avidin and alpha-glucosidase have been reported to non specifically bind to CNTs [20]. BSA was dissolved in 10mM aqueous solution of PBS (1X, pH 7.4). The solution was introduced into the microchannels and were allowed to incubate in the channels for 60 minutes. It is essential that protein solution does not flow for the proteins to bind to the CNTs. The adsorption of proteins to CNT surface was due to hydrophobic interactions between the CNTs and the proteins. This Non Specific Binding (NSB) of proteins to CNTs is irreversible.

The resisatnce of the CNT thin films were measured before and after the attachment. It was observed that, for protein concentrations of 1nM and up ward there was an increase in the resistance of the CNT thin films. The change in resistance of the CNTs maybe due to carrier scattering by the dipole present of the proteins. However, a general mechanism explaining this effect is yet to be elucidated. For BSA concentrations 1-10 nM the resistance increased . There was virtually no appreciable change in resistance for 0.1nM BSA.

BSA Conc. (nM)	**Resistance before BSA attachment (Ω)**	**Resistance after BSA attachment (Ω)**
10^{-3}	55	55
10^{-2}	55	55
10^{-1}	55	55
1	55	59
10	55	67

Table 1: Resistance change due to protein adsorption

Once the protein adsorption is complete, the device was rinsed with DI water. Once the buffer solution has been rinsed out of the channel, we begin testing the device using 0.1M HCl. It should be noted that the isoelectricpoint of BSA (the pH range betwwen which there is no net charge on the protein) is between pH 3-5. When HCl of pH 1 is introduced into the channel, the hydronium ions react with the OH^- ends of the dipoles present on the BSA leaving the BSA with a net positive charge. The test fluid (0.1M HCl) was flowed at different flow rates and the resultantant voltage was measured. Proteins of different concentrations were bound to a single CNT flow sensor of 55 Ohm resistance.

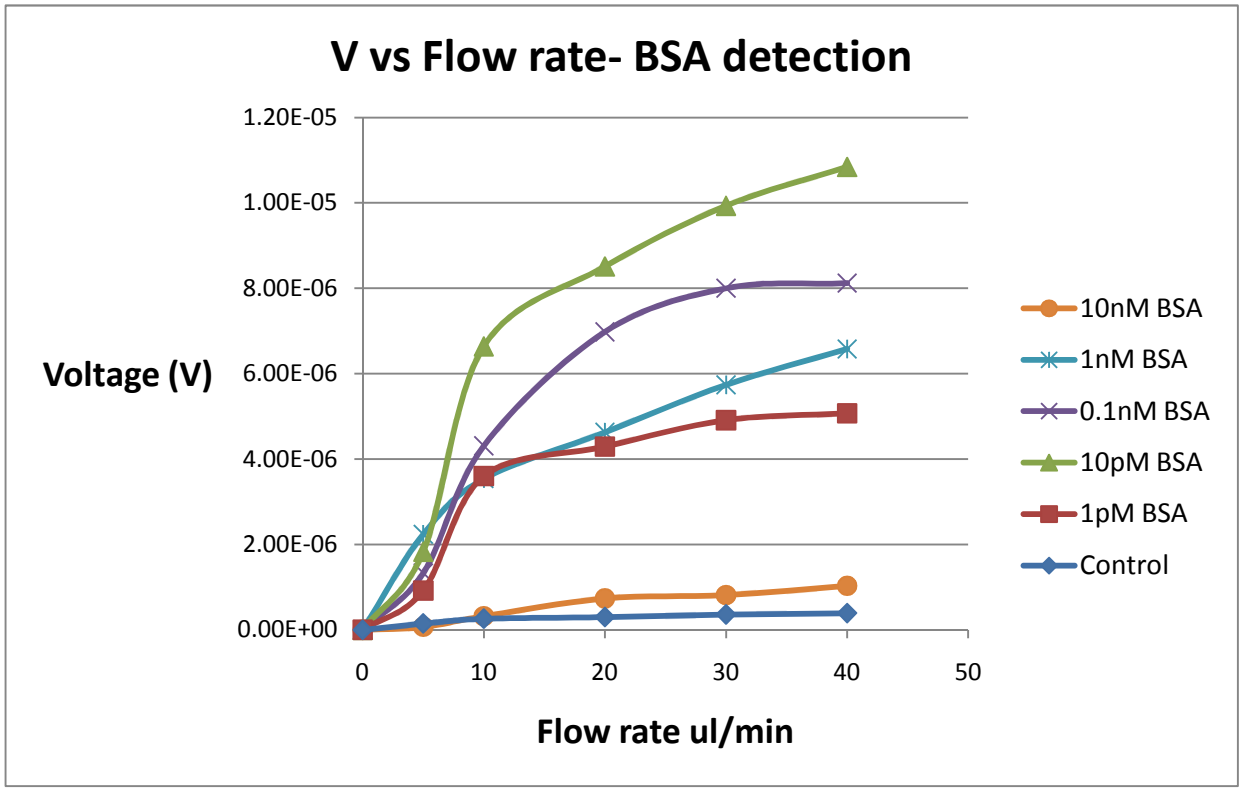

Fig16: Voltage vs Flow rate for different concentrations of BSA

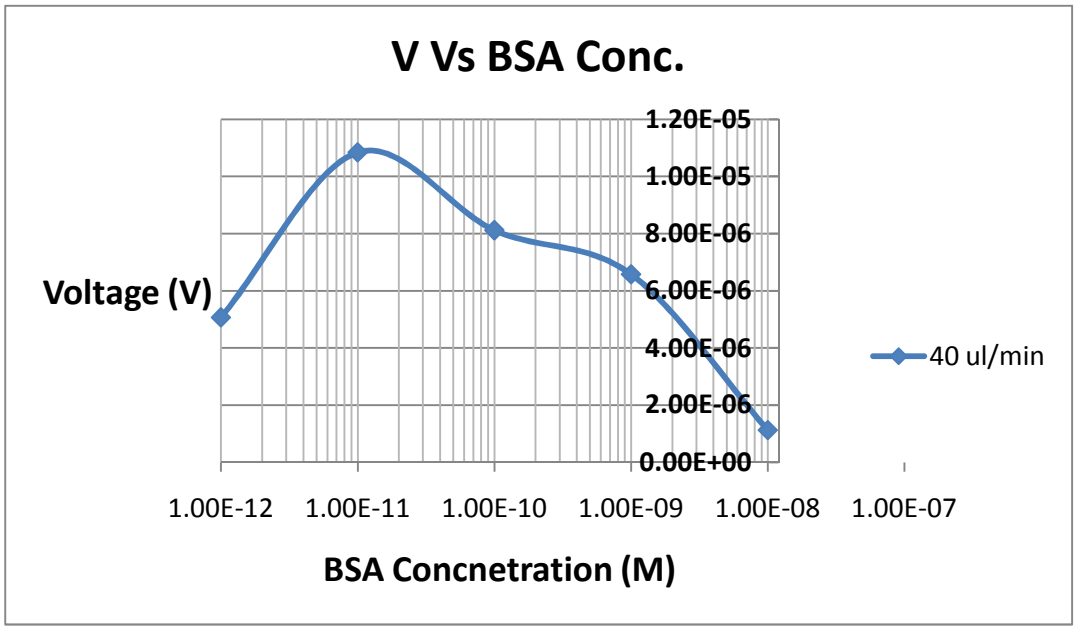

Fig 17: Voltage Vs BSA concentration

In Fig, we see the flow voltage generated for different flow rates at different BSA concentrations attached to the CNT surface. A remarkable aspect of this experiment is that the flow voltage generated after protein attachment to the CNT films are an order of magnitude higher than for the case when no protein was attached on the CNT fims (see control, Fig). We have already established that the flow generated voltage vs resistance characteristic are linear and hence even with a resistance increase due to protein adsorption (which is not an order of magnitude increase), the voltage increased by an order of magnitude. This appears to be a rather strange yet remarkable phenomenon.

For BSA concentrations 1pM, 10 pM and 100 pM (0.1nM), there is no significant increase in resistance yet a very large voltage signal has been obtained. In Fig, we see that the voltage peaks for 10pM BSA concentration (~ 11μV) . As the attachement concentration of BSA is increased the voltage begins to drop. However, even along the dropping trent i.e for BSA concentrations higher than 10pM BSA, the signal obtained are much higher than those before the attachment of BSA. Similarly, for a concentration 1pM, the volatge generated is smaller than that for 10pM but

still significantly larger than the control. The device seems to be a more sensitive around the 10pM BSA range. The decreasing senstitvity for an increasing BSA concentration is a singular aspect of this experiment.

One can only begin to venture a guess to explain this unique phenomenon. A concrete theory as of now cannot be elucidated without further experimental evidence. Only further experimental investigation will fully clarify our position on this phenomenon.

Chapter 6

Summary

As a part of this work CNT flow sensors have been integrated into microfluidic systems for flow sensing and biomolecular detection. Experiments conducted on flow sensors fabricated using Pad electrode and IDE configurations have provided some useful insights into the underlying principle based on which CNT flow sensors work. The work can be summarized as follows

- The flow induced voltage increases as the concentration of the electrolyte used increases.
- The possibility of CNT flow sensors operating based on an electrokinetic mechanism has been explored. The linear Voltage vs resistance characteristics do not seem to favor this mechanism.
- Preliminary protein detection was conducted using the CNT flow sensor by non specifically binding BSA proteins to the CNT film surface. The current induced in the CNT film is much higher than without the BSA at low concentration of the proteins (eg 1pM-10pM). The induced current decreases with increasing protein concentration.

Future Scope:

Experimental evidence seems to suggest that the CNT flow sensor's sensitivity increases as the concentration of the proteins adsorbed decreases. It remains to be seen as more experiments have been planned wherein extremely low concentration of proteins are going to bound to the CNT surface. Should this be true then an all round improvement of the flow sensor could detect femto moles of concentrations of biomolecules. Considering the fact that the flow sensor can continuously measure the flow induced voltage due to low concentrations of adsorbed proteins,

the device could be incorporated into a continuous health monitoring system, it can be of great importance to study biomolecular dynamics over large periods of time and with the optimal concentrations of biomolecules bound to the CNT film, one can characterize very small flow velocity with great sensitivity.

The flow induced voltages of liquids with a wide range of pH must be studied using the flow sensor on pad electrode configuration in order to experimentally determine the direct co-relation between pH and induced flow voltage.

Lastly, further experimental evidence is needed to definitively prove some of the tentative explanations given in this report. The explanations are meant to be “toy models” to gain some insight into the working principle of the phenomena discussed but for a comprehensive theory to be constructed, further control experiments with several other parameters have to be incorporated.

References

1. Tschulena et al., sensormagazin, 1995, 1, 1-4.
2. N.Okulan et al., A new pulsed mode micromachined flow sensor for integrated microfluidic system, in Solid State Sensor and Actuator, Hilton Head island, SC, 1998.
3. E.Meng et al, A MEMS body fluid flow sensor, in Micro Total Analysis System 2011.
4. H Ernst et al., Sens. Actuator, A., 2002, 100 (1),54.
5. J.A. Wu et al., Sens. Actuators, A., 2002, 97-98, 68-74.
6. T. Nakgama et al., Analyst, 2003, 128 (6), 543-546.
7. K.D. Caldwell et al., Anal. Chem., 1986, 58, 1583-1585.
8. M. Wang et al., Meas. Sci. Technol., 2002, 13, 1884- 1889.
9. S. Ghosh et al, Science 299, 1042-44 (2003).
10. P. Kral, M.S. Shapiro, Phys. Rev. Lett. 79, 5082 (1997).
11. B.N.J.Persson et. al, Phys.Rev. B 69,235410 (2004).
12. H. Cao et al., Microsyst Technol (2010) 16:955- 959.
13. Y. Zhou et al., App. Phys. Lett. 88, 123109 (2006).
14. M.E. Spotnitz, J. Mate. Chem, 14 (2004).
15. A.K. Tan, Bio-Rad Labs, Technote 2134
16. Bodas et al, Sensors and Actuators B 123 (2007) 368- 373.
17. S.Ghosh et al., Phys.Rev B 70, 205423 (2004)
18. Sven.H. Behrens et al., J.Chem.Phys 115, 6716 (2001)
19. Adam.E.Cohen, Science 23,1235 (2003)
20. Robert. J. Chen et al., PNAS, Vol 100, 9 (2003)

Appendix

1. LabVIEW block diagram:

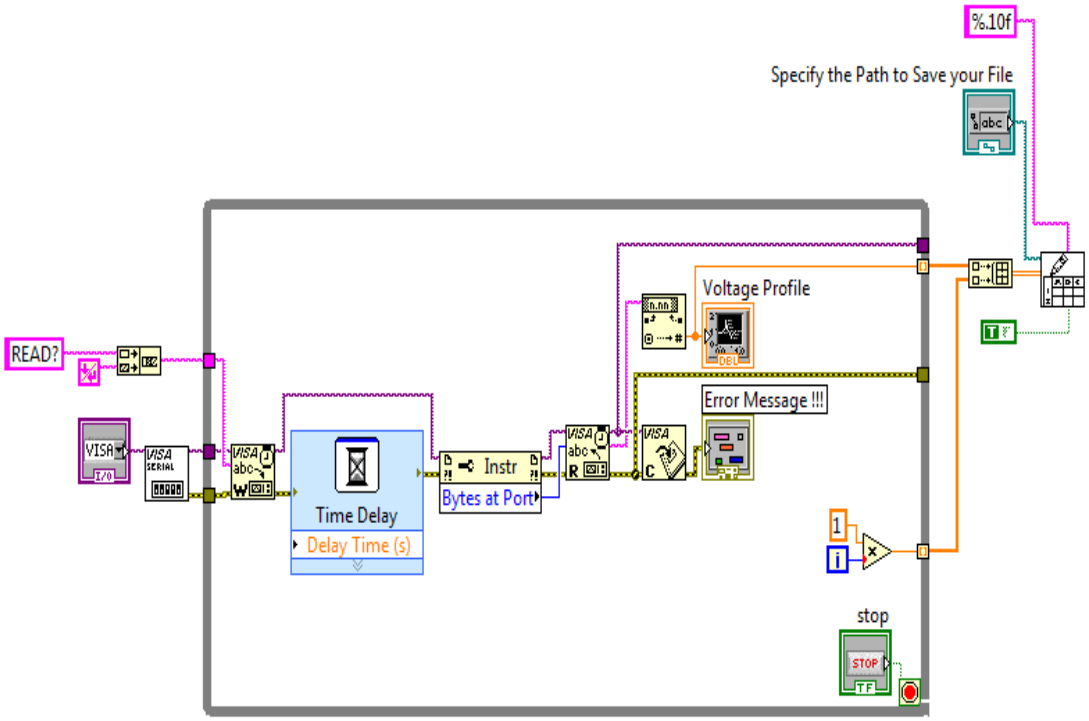

2. Material Specifications:

1. Carbon Nanotubes (CNTs) - As prepared, 40% pure, Carbon Solutions Inc.
2. Sodium Dodecyl Sulfate (SDS)- 99+% pure, A.C.S Reagent, Sigma Aldrich
3. Sylgard 184, Silicone Elastomer Kit, Curing Agent.
4. Syringe Pump- picopump, KD Scientific
5. Syringe- 1 ml, Gastight® #1001, Hamilton co.
6. Nanovoltmeter- Agilent 34420A
7. L8- 70M Ultracentrifuge, Beckman
8. Branson Sonifier 250 (Tip type Sonicator).
9. Micropipette, 10μL, Eppendorf Research
10. Albumin, from Bovine Serum, A3294- 10G, Sigma Aldrich
11. Hydrochloric Acid, 37%, A.C.S Reagent, Sigma Aldrich
12. PBS tablets, Calbiochem, EMD Biosciences, CA.
13. Acetone, BDH, BDH 2025- 1GLP, VWR Intl.
14. 2- Propanol, CAS 67-63-0, VWR Intl.
15. Methanol, Laboratory grade, A411-4, Fisher Scientific.
16. Silver Conductive epoxy, Cat No: 8331- 14G, MG Chemicals.
17. NanoPURE Diamond, Barnstead.

3. PDMS PROTOCOL:

1. Use DRIE or SU-8 to make Si wafer mold.
2. Things to start with:
   a) PDMS kit.
   b) Molding jig (1 plastic ring, 1 plastic plate)
   c) Clamps for the jig
   d) Square thick glass plate with both surface flat and clean
   e) Beaker
   f) Spatula
3. Turn on the convection oven.
   a) Determine real working temperature of the oven using a thermometer.
   b) Check for the flatness of the shelf and make adjustment if needed.
   c) Set the temperature to be 80°C so that the temperature on the shelf will be around 70°C.
   d) Place supporting plate between the molding jig.
4. Weigh ten parts of the Silicone elastomer to one part Curing agent by weight in a glass beaker.
   a) When using the jig, 35g of mixed PDMS will give you about 3mm thick PDMS. Weigh 25% more (45g) to account for the left-over in the beaker in this case.
5. Violently mix them with a spatula for ten minutes. (Optional) let it sit for ten minutes to reduce the bubble.
6. Use a vacuum chamber to degas.
   a) Always put the beaker inside a secondary container (e.g. a large Petri dish) to prevent overflows PDMS from contaminating the chamber.
   b) Start the vacuum slowly.
   c) In case of a potential overflow, turn on the vent a little bit.
   d) When there are very few bubbles, turn off the pump then vent slowly.
7. Prime the wafer and molding jig with HMDS.
   a) This should be performed in vacuum chamber. The vacuum chamber and vacuum pump should be inside fume hood.
   b) Assemble the jig with clamps. Put the wafer mold at the center of the jig. Place the HMDS vial on the other side of the vacuum port, and open the cap to allow evaporation.
   c) Start the pump slowly and pump for 3 minutes, then stop the pump and vent slowly.
      Note: This step is critical for preventing PDMS stiction to mold. In general if PDMS sticks to mold, the mold is destroyed. Make sure the mold is clean. (Optional) For reusing the mold, do a PEII oxygen plasma descum before priming.
8. Pour degassed PDMS onto the mold as fast as you can to avoid excessive bubbles. If the PDMS thickness needs to be tightly controlled, this step can be performed on a scale. Use two pipette tips to push bubble on surface to outside and try to drive the air between mold and Petri dish out.
9. Put the jig assembly on the flat thick glass plate inside the convection oven. Bake at 80°C for 25 minutes. During this time, clean the mixing beaker with IPA. Also clean the vacuum chamber if you made any spill.

Note:

a) You need to monitor the oven temperature before you put the PDMS with mold in. Remember the oven temperature is not uniform and plastics (Petri dish for example) will deform significantly above 90°C.
b) You need to make sure the mold is as horizontal as possible to ensure uniform PDMS thickness.

10. Separate mold from cured PDMS carefully along the designed channels. Use razor blade to cut the PDMS into pieces.

4. Time trace of Flow generated voltage, SNR.

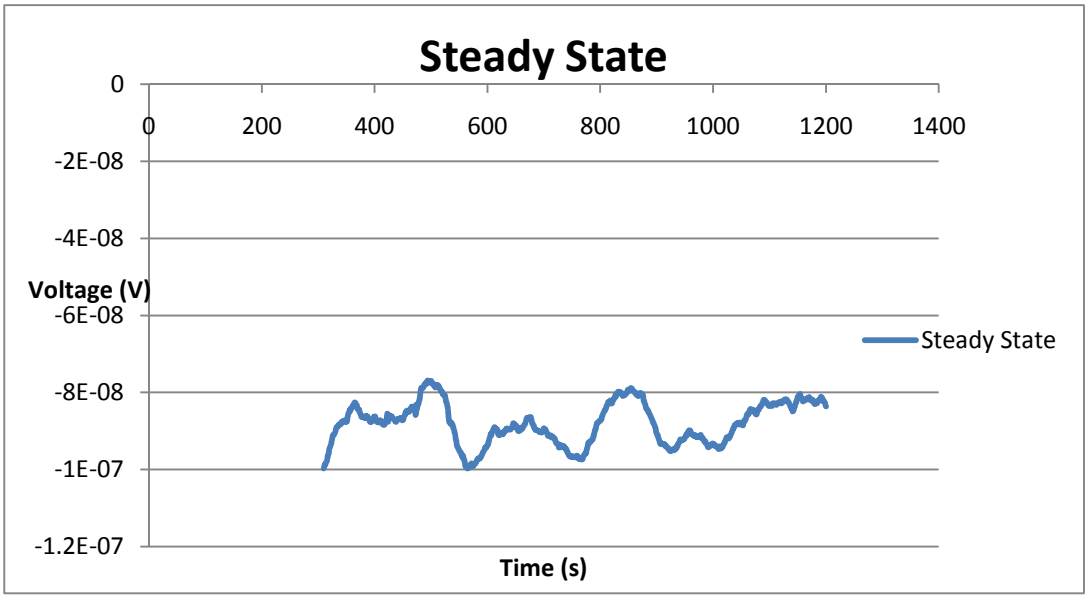

Figure 1: Steady state noise at no flow. Mean: -87.8 nV, Standard Deviation: 5.4 nV

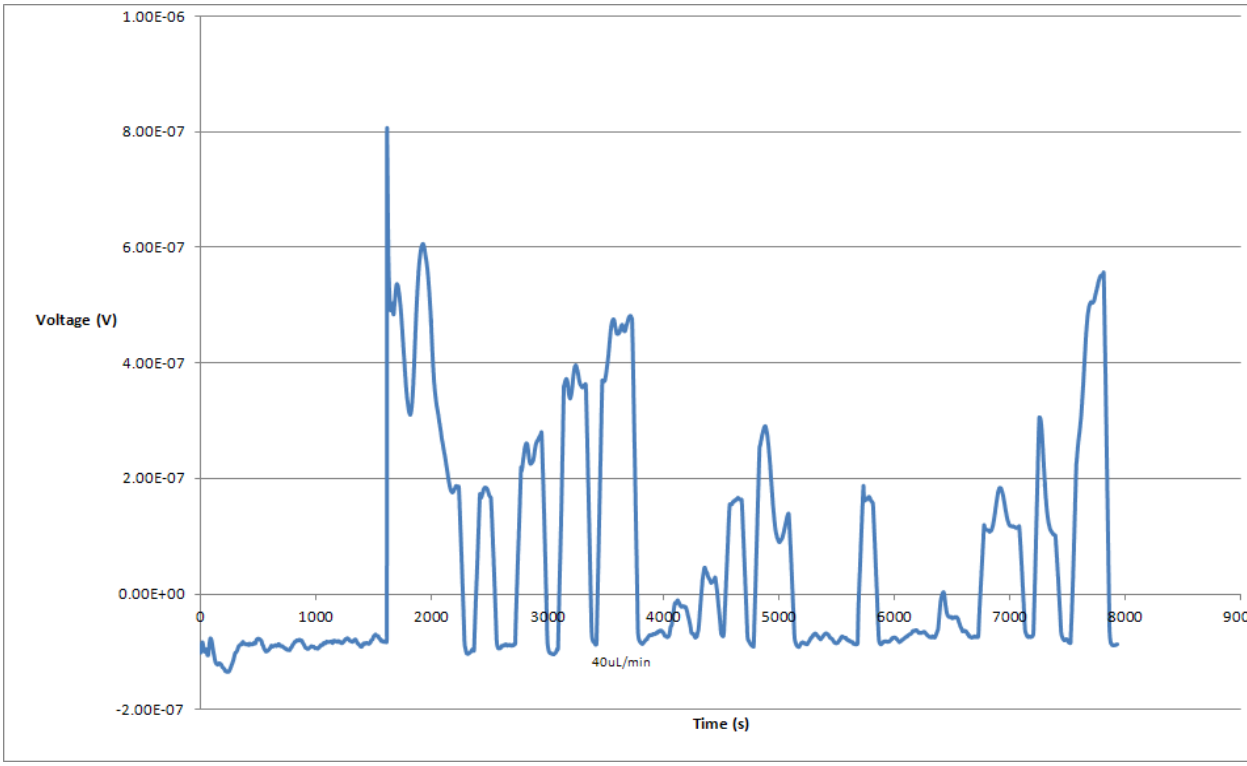

Figure 2: A time trace of generated volatge in a 72 ohm sensor with 0.1M HCl. At 40µL/min, the Voltage generated is 560 nV. Hence, the Signal to Noise Ratio (SNR) is 560 nV/5.4 nV = ~ 104 at 40 µL/min.